Canadian Mineralogist
Vol. 31, 203-217 (1993)

COMPOSITION AND COLOR OF BIOTITE FROM GRANITES: TWO USEFUL PROPERTIES IN THE CHARACTERIZATION OF PLUTONIC SUITES FROM THE HEPBURN INTERNAL ZONE OF WOPMAY OROGEN, NORTHWEST TERRITORIES

ANDRÉ E. LALONDE

Centre Géoscientifique Ottawa–Carleton, Université d'Ottawa, Ottawa, Ontario K1N 6N5

PIERRE BERNARD

Institut National d'Optique, Sainte-Foy, Québec G1V 4C5

ABSTRACT

A combined compositional and optical spectrophotometric study of 24 biotite specimens from the granitic rocks of the Hepburn and Bishop intrusive suites of the early Proterozoic Wopmay orogen, Northwest Territories, shows that the chemical composition and the color of this mineral strongly reflect the tectonic origin of its host. In the continental-collision-related Hepburn suite, biotite is enriched in total Al and Fe and is Fe^{3+}-poor, consistent with anatexis or assimilation of reduced metasedimentary material. In the Bishop suite, formed within a continental arc, biotite is Al-poor, Mg- and Fe^{3+}-rich, indicating relatively more oxidizing conditions and a less important metasedimentary contribution. The biotite quadrilateral (annite – siderophyllite – phlogopite – eastonite diagram) effectively portrays the compositional trends of micas from continental-collision- and arc-related granites. The bright red color of biotite from peraluminous collisional granitic plutons reflects a high total Fe content with low $Fe^{3+}/(Fe^{2+}+Fe^{3+})$, and probably also the presence of Ti^{3+}. Green or brown biotite from arc-related granites is Mg- and Fe^{3+}-rich.

Keywords: biotite, mica, peraluminous granites, continental collision granites, arc-related granites, pleochroism, spectrophotometry, Wopmay orogen, Northwest Territories.

SOMMAIRE

Nous avons documenté la composition chimique et le spectre de transmission optique de 24 spécimens de biotite obtenus des roches granitiques des suites intrusives de Hepburn et de Bishop, situés dans l'orogène protérozoïque de Wopmay, dans les Territoires du Nord-Ouest. La composition chimique et la couleur pléochroïque de ces micas sont des indicateurs du milieu tectonique de leur roche-mère. Dans la suite Hepburn, produite par une collision continentale, la biotite est enrichie en Al et en fer total et est appauvrie en Fe^{3+}, témoignant d'une origine par anatexie de matériau métasédimentaire réduit. Dans la suite Bishop, formée dans le cadre d'un arc continental, la biotite est enrichie en Mg et Fe^{3+} et appauvrie en Al, indiquant des conditions plus oxydantes et une pénurie de matériau métasédimentaire. Le quadrilatère de la biotite (annite – sidérophyllite – phlogopite – eastonite) permet de distinguer clairement les lignées des suites collisionnelles de celles des arcs continentaux. Un fort enrichissement en fer total, un faible rapport $Fe^{3+}/(Fe^{2+}+Fe^{3+})$, et possiblement aussi la présence de Ti^{3+} seraient à l'origine du pléochroïsme rouge vif de la biotite des granites hyperalumineux collisionnels. La biotite verte ou brune des granites des arcs est enrichie en Fe^{3+} et Mg.

Mots-clés: biotite, mica, granites hyperalumineux, granites de collision continentale, granites d'arcs continentaux, pléochroïsme, spectrophotométrie, orogène Wopmay, Territoires du Nord-Ouest.

INTRODUCTION

Petrologists have recently devoted considerable effort to the elaboration of geochemical or petrological schemes of classification of granitic rocks (*e.g.*, Barbarin 1990). These, in turn, have been more or less successfully associated to various magmatic processes and tectonic settings. In many of these schemes, peraluminosity and relative state of oxidation of a magma play essential roles. For example, in their investigation on the I- and S-type granites of Australia, Chappell & White (1974) emphasized how a high peraluminosity indicates derivation by partial melting of a crustal sedimentary (S-type) source, in contrast to low peraluminosity for granites derived by partial melting of an igneous (I-type) source. Similarly, Ishihara (1977, 1981) characterized the granitic rocks of Japan as belonging to the ilmenite and magnetite series, depending on their Fe–Ti oxide mineralogy and magnetic susceptibility, both reflections of their relative state of oxidation.

In view of this, it is surprising that the composition of biotite has not been used more actively in the classification of granites, since this ubiquitous mineral is by far the most important host of any excess aluminum in granites; furthermore, it is the most readily available indicator of oxidation state [$f(O_2)$]. Recent studies by Nachit *et al.* (1985) and Ague & Brimhall (1988) have certainly demonstrated the potential of using biotite as a petrogenetic and tectonomagmatic indicator in granites. Therefore, classifications of granitic rocks based on peraluminosity or oxidation state could gain much by considering the composition of biotite.

In this paper, the composition and color of biotite from two petrologically, chronologically and tectonically distinct intrusive suites from the internal zone of the early Proterozoic Wopmay orogen in the Northwest Territories are described. The study has two principal objectives. First, to illustrate how the composition and pleochroism of biotite reflect the oxidation state and the peraluminosity of granitic rocks. Second, to demonstrate how these properties can help to discriminate continental collision and arc-related granitic suites in the early Proterozoic Wopmay orogen, and also other complex orogenic belts.

Regional Geology

The geology and tectonic evolution of the Wopmay orogen are briefly summarized below. St-Onge & King (1987) and Hoffman *et al.* (1988) have provided detailed accounts.

The 1.9 Ga Wopmay orogen is a small (300 × 500 km) orogenic belt that unconformably flanks the northwestern edge of the Archean Slave craton in the northwest corner of the Canadian Shield. Three principal tectonic elements are defined (Fig. 1) (Hoffman & Bowring 1984); from east to west, they are the Coronation prism, the Great Bear magmatic zone, and the Hottah terrane. These three elements are described below. In the easternmost part of the Wopmay orogen is the west-facing *Coronation prism*, comprised of rift-fill, passive margin, and foredeep sequences, which are collectively named the Coronation Supergroup. In the western portion of the Coronation prism, these units have been thrust onto Archean basement, translated eastward along a ductile sole-thrust, folded, intruded and metamorphosed by the Hepburn intrusive suite during the collisional Calderian orogeny (King 1986) at *ca.* 1.885 Ga (Hoffman & Bowring 1984). This deformed part of the prism is the Hepburn metamorphic–plutonic internal zone (HMIZ, Fig. 1). To the east of the HMIZ, the ductile sole-thrust fans into a series of thin-skinned imbricate thrust-slices, which constitute the Asiak fold-thrust belt (AFTB, Fig. 1). Still further east, Coronation units lie autochthonously upon the basement. The second tectonic element in the westernmost part of the orogen is the *Hottah terrane* (HT, Fig. 1). It is composed of high-grade metamorphic rocks intruded by a 1.914 to 1.900 Ga calc-alkaline arc (Hildebrand *et al.* 1987). Finally, located in the center, between the Hottah terrane and the Coronation prism, is the third tectonic element of the orogen, the *Great Bear magmatic zone* (GBMZ, Fig. 1), a younger (1.878 to 1.848 Ga) volcanic–plutonic arc that unconformably overlies the Hottah terrane to the west and the HMIZ to the east, and presumably resulted from inferred east-dipping subduction of oceanic lithosphere west of the Hottah terrane (Hildebrand *et al.* 1987, Hoffman & Bowring 1984).

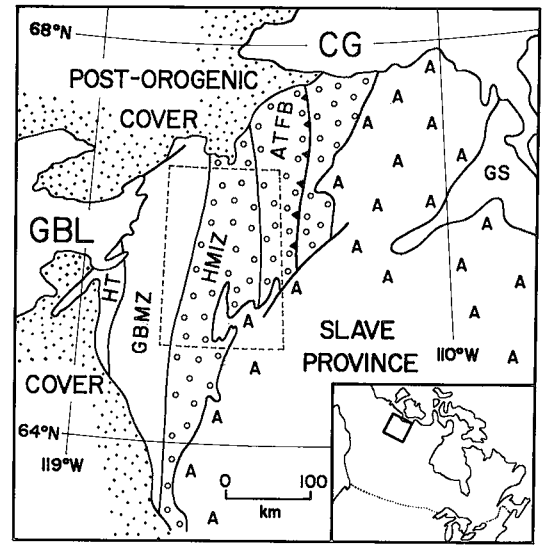

FIG. 1. Location map of Wopmay orogen; dashed-line rectangle outlines study area. Principal tectonic zones: HT Hottah terrane, GBMZ Great Bear magmatic zone, HMIZ Hepburn metamorphic–plutonic internal zone, ATFB Asiak thrust-fold belt. Circles denote the Coronation Supergroup; other symbols: GS Goulburn Supergroup, CG Coronation Gulf, A Archean basement, GBL Great Bear Lake.

Plutonic Suites of the Hepburn Internal Zone

The biotite separates studied in this project come from two petrologically, geochemically and chronologically distinct plutonic suites within the HMIZ (Fig. 2): the dominantly peraluminous continental-collision-related Hepburn intrusive suite (Lalonde 1989), and the subduction-related Bishop intrusive suite (Lalonde 1989). Plutons within the HMIZ also define two north-trending belts (Fig. 2). The easternmost belt, roughly 200 km long and up to 40 km in width, is composed *solely* of plutons of the Hepburn intrusive suite. The narrower and less continuous western belt is composed of plutons from both Hepburn and Bishop intrusive suites.

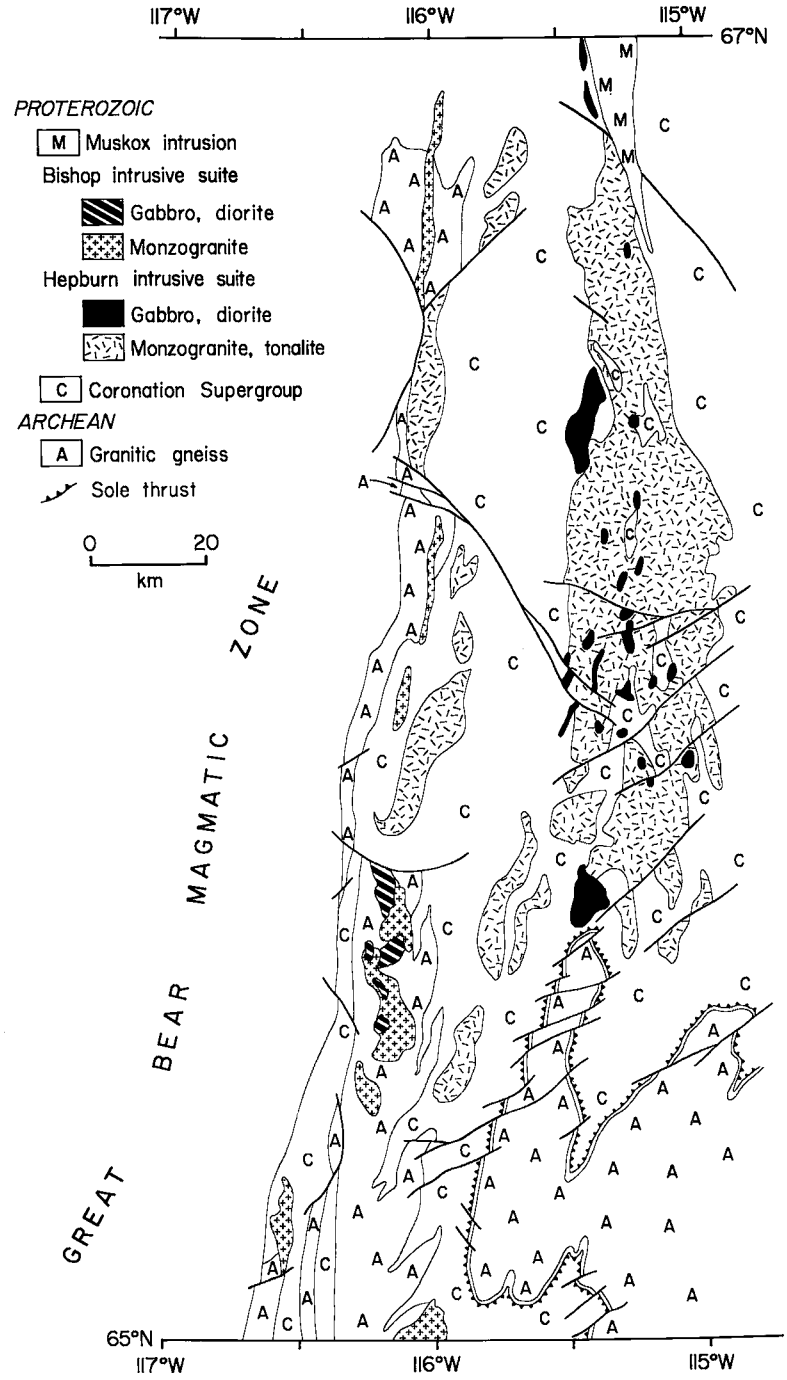

FIG. 2. Simplified geological map of plutonic units (from Lalonde 1986). Dark lines trending northeast or northwest indicate late regional transcurrent faults.

The older 1.890 to 1.878 Ga Hepburn intrusive suite varies continuously in composition from gabbro to granite, but peraluminous granites are dominant. The gabbroic rocks include small plutons and dikes of norite, gabbro, and diorite that show evidence of synplutonic emplacement with respect to granite. Although of limited areal extent, the mafic rocks imply a mantle contribution to the suite. The granites form considerably larger plutons of biotite–muscovite granite with large (~5 cm, long axis) euhedral megacrysts of white microcline, xenocrysts of garnet and porphyroblasts of sillimanite. Fe–Ti oxides are almost always absent; only in a few instances was ilmenite observed. The older granites of the Hepburn suite are synmetamorphic. They have a moderate foliation, and abundant schlieren and xenoliths of metasedimentary material, and show nebulous contacts with their metamorphosed pelitic host-rocks. The younger granites are massive, less migmatitic, and may have chilled margins and a thermal aureole. Plutons of the Hepburn intrusive suite, especially those in the eastern belt of plutons, were thrust eastward over the basement while still hot (St-Onge & King 1987).

The younger 1.848 Ga Bishop intrusive suite is, much like the Hepburn suite, also composed of a spectrum from gabbro to granite. However, the granites from this suite are characterized by biotite and hornblende. They also have considerable amounts of titanite as an accessory phase, are magnetite-bearing and ilmenite-free, and have pink or red, hematite-clouded megacrysts of K-feldspar, all features indicative of oxidizing magmatic and postmagmatic conditions (Lalonde 1989). In contrast to their Hepburn counterparts, all of the Bishop plutons intruded the underlying Archean basement and were not tectonically transported before the end of their cooling. They are in sharp contact with their high-grade host-rocks and commonly display chilled margins.

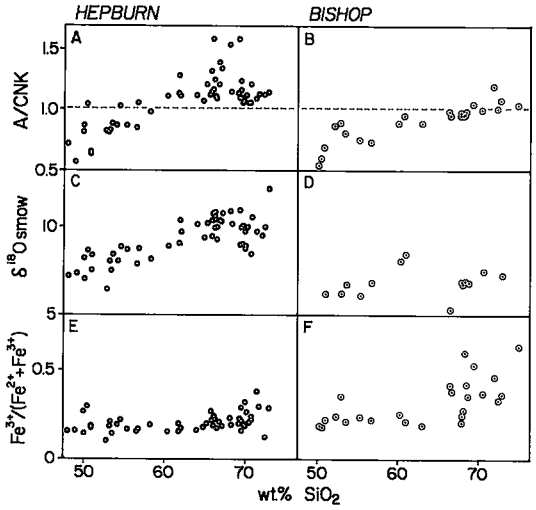

FIG. 3. Geochemistry of the Hepburn and Bishop intrusive suites. Plotted against wt.% SiO_2 are peraluminosity [A/CNK = molar $Al_2O_3/(CaO + Na_2O + K_2O)$], whole-rock $\delta^{18}O$ and $Fe^{3+}/(Fe^{2+}+Fe^{3+})$ values for Hepburn and Bishop units. Oxygen isotope ratios are expressed relative to standard mean ocean water (SMOW). Points plotting above dotted line (A/CNK = 1) in Figures 3A and 3B are peraluminous. Heavy circles and light circles with central dots represent Hepburn and Bishop data, respectively. These symbols are also used in following figures.

Since both suites range from gabbro to granite, they share many characteristics. Some compositional indices nevertheless set the two suites apart, and these reflect differences in their petrogenesis. For example, the units of the Hepburn intrusive suite show, in contrast to the Bishop units, a pronounced peraluminosity, as expressed by the molar ratio A/CNK [= $Al_2O_3/(CaO + Na_2O + K_2O)$], and $\delta^{18}O$ with increasing silica (Figs. 3A and B, 3C and D, respectively), both indications of the increasing importance of the metasedimentary contribution to the felsic members of the suite. In addition, the Hepburn rocks do not show any signs of late oxidation of iron, as do the Bishop rocks (Figs. 3E, F), presumably because conditions were kept reducing in the Hepburn rocks by the presence of graphite in the incorporated metasediments. The strong oxidation of iron in the most felsic Bishop units (Fig. 3F) may represent the cumulative effect of hydrogen loss upon water saturation in the absence of graphite as a reducing agent (Czamanske & Wones 1973).

Occurrence of Biotite

Biotite is the principal mafic mineral of the granitic rock-units of both the Hepburn and Bishop intrusive suites. The mineral also occurs in the gabbroic and dioritic rocks of these two suites. In this section, the mode of occurrence and the textural relationships of the biotite are described separately for both.

In the mafic units of the Hepburn suite, biotite is found as small ragged subhedral crystals, $\leq$ 1.5 mm across, clustered with pyroxene, amphibole and opaque oxides. In these clusters, the mineral clearly rims and replaces pyroxene or amphibole, and originated most likely by late deuteric hydration of these primary ferromagnesian silicates. Minor amounts of biotite crystallized from pockets of residual volatile-enriched magma.

In the Hepburn granitic rocks, biotite is the dominant ferromagnesian mineral. Other mafic minerals such as garnet, tourmaline, chlorite and ilmenite may occur, but only in trace amounts. Two texturally distinct groups of biotite are recognized, associated respectively with the older foliated granites and the younger massive granites. In the foliated units, subhedral flakes of biotite up to 2 mm across are interstitial to the large megacrysts of feldspar and define the faint to moderate planar metamorphic fabric of the rock. Evidence of strain comes

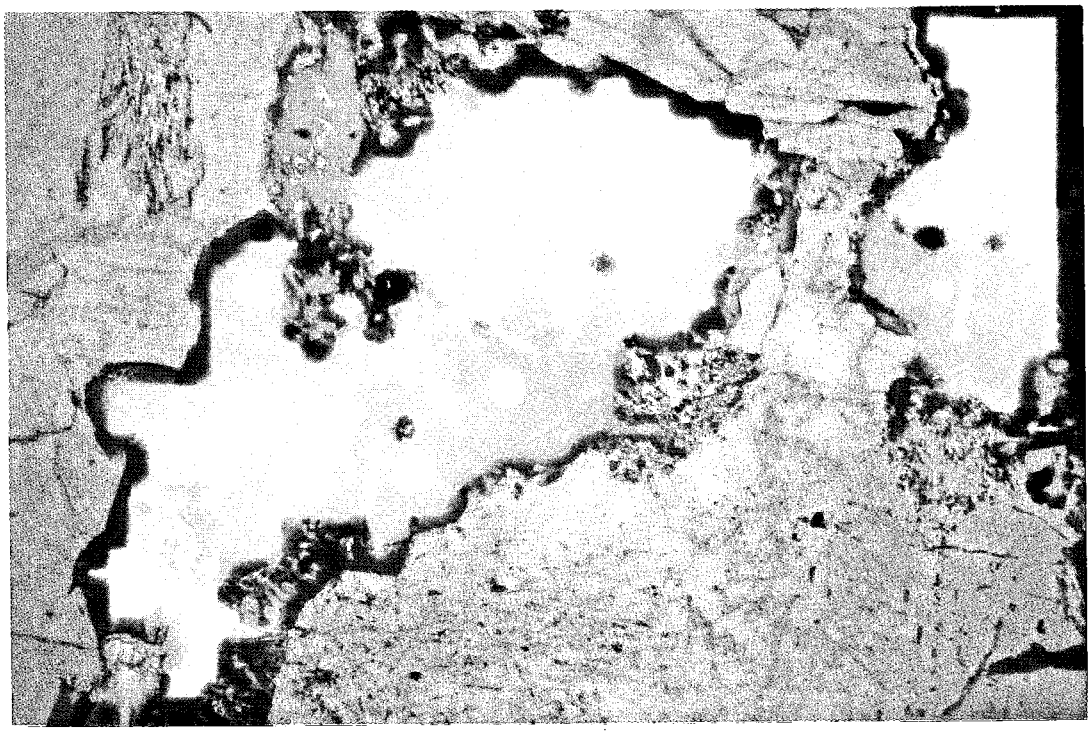

FIG. 4A. Photomicrograph of reddish brown biotite in Hepburn granite L341A. Note pleochroic halos surrounding zircon crystals. Plane-polarized light; field of view: 3.3 mm.

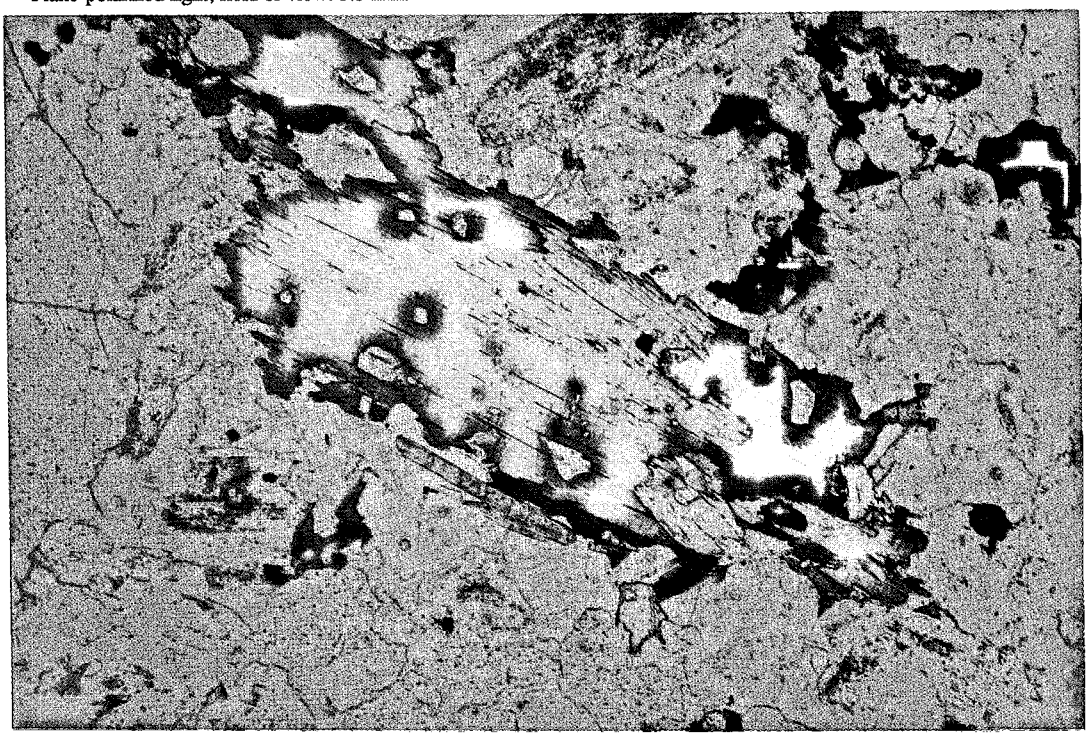

FIG. 4B. Photomicrograph of green biotite in Bishop granite L246. Plane-polarized light; field of view: 3.3 mm.

from the bending of the cleavage, commonly around crystals of garnet. In addition to metamorphic recrystallization, some of these crystals also show evidence of late alteration, such as prehnite–carbonate exfoliation lenses (Phillips & Rickwood 1975) and disseminated opaque dust, generally concentrated along the cleavage.

In contrast, biotite in the younger massive units of the Hepburn suite invariably is interstitial to the large megacrysts of feldspar, with the subhedral to euhedral flakes reaching up to 4 mm across and showing no evidence of strain or opaque dust. In these rocks, the mineral is interpreted as being primary. All grains of biotite have inclusions of apatite and zircon, the latter with a pleochroic halo (Fig. 4A). Such biotite is pleochroic from yellow or straw to deep reddish brown (Fig. 4A).

Unlike biotite in the Hepburn suite, biotite in the granitic units of the Bishop intrusive suite usually is not the only mafic phase. It generally occurs as small ragged anhedral flakes $\leq$ 1.5 mm across, but larger isolated crystals up to 3 mm across also are observed. It occurs with roughly equal proportions of subhedral to euhedral amphibole along with magnetite, apatite, titanite and allanite (Fig. 4B). Although some of the small crystals of biotite clustered with amphibole could have originated in part by postmagmatic replacement of the amphibole, the well-defined planar boundaries between these two minerals suggests that they crystallized from a residual volatile-enriched magma. Biotite in the Bishop granites is pleochroic from golden yellow to dark greenish brown (Fig. 4B). As is the case of the Hepburn plutons, inclusions of apatite and zircon are widespread in the biotite. In the gabbroic units of the Bishop suite (sample L316), biotite occurs as large poikilitic crystals up to 4 mm across and encloses pyroxene. This biotite, in contrast to that in the other Bishop samples, is deep-red pleochroic, and is a late-crystallizing phase, partly replacing the earlier primary pyroxene.

Analytical Methods

Biotite from 24 fresh and representative samples of the plutonic rocks, mostly granites, was studied, 13 from the Hepburn intrusive suite, and 11 from the Bishop intrusive suite. The biotite was analyzed for the major elements, fluorine, and chlorine by wavelength-dispersion X-ray spectrometry with the Camebax electron microprobe of the McGill University Microprobe Laboratory. X-ray counts were accumulated simultaneously on four spectrometers, with a beam accelerating potential of 15 kV and a current of 7 nA. ZAF corrections and data reduction were performed with the on-board software package supplied by Cameca. Statistics compiled from repeated analyses of a biotite standard are given in Appendix 1. In addition, biotite was separated by combined magnetic and heavy-liquid methods from six samples of the Hepburn granite and seven of the Bishop granite. These samples were chosen principally because of the large volume of rock available, but also for representativity. The samples of biotite separated were 97% pure or better, with the remainder being mostly plagioclase or heavy accessory minerals such as zircon, allanite and titanite. The samples were then analyzed three times for Fe^{2+} and Fe^{3+} by the standard Wilson titration method (Wilson 1955). For those samples not measured, the $Fe^{3+}/(Fe^{2+}+Fe^{3+})$ ratios were extrapolated from those of the similar petrographic units.

Optical transmission spectra of five samples of Hepburn and seven samples of Bishop biotite were acquired with plane-polarized light for the *Z* vibration direction using a custom-designed visible to near-infrared (VIS–NIR) optical spectrophotometer. The instrument consists of a Zeiss Jena Amplival polarizing microscope coupled to a 0.75 m *f*7.5 Spex grating monochromator and Xe arc source. Intensity measurements were done with a side-window VIS–NIR photomultiplier tube attached to the accessory head of the microscope. Stray-light interference was eliminated by modulating the monochromator output with an optical chopper and filtering the signal with an associated lock-in amplifier. Spectra were analyzed with a personal computer interfaced with the amplifier. All spectra were acquired from crystals in 30-μm-thick polished sections, oriented with the {001} cleavage parallel to the stage. Given the nearly uniaxial character of the biotite, discrimination of the *Y* and *Z* vibration directions was in many cases difficult. Absorption for the *Y* and *Z* directions is nearly identical. Finally, the intensities measured were corrected for spectral variation in the intensity of the light source.

Composition of Biotite

The compositions and structural formulae of the 13 samples of Hepburn and 11 of Bishop mica are presented in Tables 1 and 2, respectively. All the mica samples consist of biotite in the sense of Deer *et al.* (1962) (*i.e.*, $Fe/(Fe+Mg) \geq 0.33$) and are trioctahedral ($5.49 < \Sigma Y < 5.77$), except for a single sample of phlogopite from a Bishop gabbro (sample L316). Despite the presence of one sample of phlogopite, the mica samples are collectively referred to as biotite in this study. Within each of the two intrusive suites, biotite displays considerable compositional variation, but is nevertheless clearly distinguished on several counts.

First, biotite in the Hepburn suite has total Al content in the range of 2.61 to 3.52 atoms per formula unit (a.p.f.u.), considerably higher than that from the Bishop suite, 2.37 to 2.62 a.p.f.u. (Fig. 5). Consequently, in all samples of Hepburn biotite, there is sufficient Al^{3+} to completely fill the tetrahedral sites, and there is an excess of Al^{3+} carried over to the octahedral sites. However, in many of the samples of biotite from the Bishop suite, there is insufficient Al^{3+} to fill the tetrahedral sites, and Ti^{4+} is required to complete the tetrahedral sites. In those samples, there is no octahedral Al^{3+}. Ti^{4+} was preferred

TABLE 1. COMPOSITION OF BIOTITE IN THE HEPBURN INTRUSIVE SUITE

ROCK-UNIT[1]	Hg2	Hq	Hg3a	Hg3a	Hg3b	Ht2	Hg3c	Hg3d	Hg3d	Ht2	Ht1	Hg2	Hg2
SAMPLE	L14	L20[2]	L86[2]	L99[2]	L125	L200	L204	L331[2]	L341A	L429[2]	L609[2]	S29	S54[2]
# OF ANALYSES[3]	8	5	10	6	6	7	8	5	4	8	10	8	3
SiO_2 wt.%	35.14	35.69	34.22	34.76	34.00	35.66	34.43	34.56	34.24	35.24	35.14	35.35	34.62
TiO_2	3.38	3.86	3.15	2.82	3.39	3.44	2.67	3.23	2.93	3.21	2.98	3.55	3.33
Al_2O_3	16.49	14.38	18.59	18.82	15.13	15.80	16.15	18.25	19.16	17.56	16.87	15.86	17.18
Fe_2O_3	2.04	1.74	1.06	1.07	1.80	1.71	1.98	1.11	1.07	1.63	1.68	2.26	2.04
FeO	21.09	21.74	20.69	20.95	26.73	22.12	23.69	21.61	20.91	21.04	21.78	21.12	19.96
MnO	0.27	0.15	0.24	0.21	0.31	0.28	0.41	0.26	0.29	0.41	0.28	0.29	0.16
MgO	7.40	9.28	7.67	7.00	4.44	6.74	6.26	5.92	6.37	7.12	7.70	7.60	7.26
CaO	0.01	0	0.03	0	0.01	0.02	0.02	0	0.01	0	0.02	0.01	0
Na_2O	0.04	0.07	0.10	0.12	0.07	0.05	0.06	0.13	0.14	0.03	0.08	0.06	0.06
K_2O	9.93	9.69	9.77	9.90	9.84	9.83	9.69	9.31	9.26	9.72	9.74	9.87	9.79
F	1.33	0.80	0.73	0.97	0.49	0.84	1.07	1.22	0.63	0.94	0.60	1.22	1.20
Cl	0.44	0.33	0.24	0.29	0.57	0.13	0.28	0.33	0.32	0.07	0.23	0.34	0.53
O≡F, Cl	0.66	0.41	0.36	0.48	0.34	0.38	0.51	0.58	0.33	0.41	0.30	0.59	0.62
TOTAL	96.90	97.32	96.13	96.43	96.44	96.24	96.20	95.35	95.00	96.56	96.80	96.94	95.51
Structural formulae based on 22 oxygens													
Si	5.440	5.492	5.282	5.355	5.441	5.545	5.433	5.404	5.333	5.422	5.416	5.468	5.407
Z=8 ^{IV}Al	2.560	2.508	2.718	2.645	2.559	2.455	2.567	2.596	2.667	2.578	2.584	2.532	2.593
^{IV}Ti	0	0	0	0	0	0	0	0	0	0	0	0	0
^{VI}Al	0.450	0.101	0.664	0.771	0.294	0.440	0.436	0.769	0.850	0.606	0.481	0.359	0.569
^{VI}Ti	0.393	0.447	0.366	0.326	0.409	0.402	0.316	0.380	0.343	0.371	0.346	0.413	0.391
Fe^{3+}	0.238	0.201	0.123	0.124	0.216	0.200	0.235	0.130	0.125	0.188	0.195	0.264	0.239
Fe^{2+}	2.731	2.798	2.671	2.700	3.578	2.877	3.127	2.827	2.723	2.707	2.807	2.732	2.607
Mn	0.036	0.019	0.031	0.027	0.043	0.037	0.055	0.034	0.038	0.053	0.037	0.038	0.021
Mg	1.707	2.130	1.764	1.608	1.059	1.563	1.474	1.379	1.478	1.634	1.769	1.753	1.689
ΣY	5.555	5.695	5.618	5.557	5.599	5.520	5.643	5.519	5.558	5.561	5.635	5.558	5.517
Ca	0.002	0	0.005	0	0.002	0.003	0.003	0	0.003	0.001	0.003	0.002	0
Na	0.012	0.020	0.031	0.037	0.023	0.014	0.020	0.040	0.044	0.010	0.025	0.017	0.019
K	1.961	1.902	1.923	1.947	2.008	1.951	1.951	1.857	1.839	1.907	1.915	1.947	1.950
ΣX	1.974	1.922	1.960	1.984	2.032	1.967	1.974	1.897	1.885	1.918	1.942	1.966	1.970
F	0.650	0.387	0.358	0.471	0.247	0.413	0.532	0.604	0.308	0.455	0.294	0.597	0.591
Cl	0.116	0.086	0.062	0.075	0.155	0.034	0.076	0.087	0.084	0.019	0.060	0.090	0.141
Fe/(Fe+Mg)	0.635	0.585	0.613	0.637	0.782	0.663	0.695	0.682	0.658	0.639	0.629	0.631	0.628
$Fe^{3+}/(Fe^{2+}+Fe^{3+})$	0.080	0.067	0.044	0.044	0.057	0.065	0.070	0.044	0.044	0.065	0.065	0.088	0.084
Al tot.	3.010	2.608	3.382	3.416	2.853	2.896	3.003	3.364	3.516	3.184	3.065	2.891	3.162

[1] Rock units as defined in St-Onge et al. (1988):
Hq Hornblende-biotite quartz diorite, diorite; minor monzogranite, tonalite, gabbro; often agmatitic and poorly foliated (may be older than Ht2).
Ht2 Biotite granodiorite; minor monzogranite, tonalite; often with marginal zone showing poikilitic K-feldspar megacrysts; weakly foliated, grey (may be younger than Hq).
Hg3 Biotite monzogranite, syenogranite; minor granodiorite; locally with large equant K-feldspar megacrysts, muscovite, garnet and sillimanite, locally with foliated edges, grey. a, McIntosh pluton. b, Keskarrah pluton. c, Rib pluton. d, Robb pluton.
Ht1 Biotite tonalite, granodiorite; locally biotite monzogranite; well foliated, grey.
Hg2 Biotite syenogranite, monzogranite; locally with large tabular K-feldspar megacrysts, muscovite and garnet, commonly with metasedimentary xenoliths; foliated, grey.
[2] FeO/Fe_2O_3 estimated from analyses of biotite in the same rock unit.
[3] Number of analyses included in mean.

over Fe^{3+} to complete the tetrahedral sites because current Mössbauer investigations of mica from the Hepburn and Bishop suites have demonstrated the absence of any tetrahedral Fe^{3+} in both Hepburn and Bishop mica (Rancourt & Lalonde, in prep., Rancourt *et al.* 1992).

Second, biotite in the Hepburn suite is systematically more Fe-rich [Fe/(Fe+Mg) values in the range of 0.59 to 0.78] than biotite in the Bishop suite (0.28 to 0.57) (Fig. 5). The biotite from Bishop sample S200, an unusual late granite, is an exception and has a Fe/(Fe+Mg) value of 0.86.

Third, although the compositions of biotite from the Hepburn and Bishop intrusive suites show some overlap in their Ti contents, biotite in the Bishop suite may attain higher Ti contents than in the Hepburn suite. Titanium contents range from 0.32 to 0.45 a.p.f.u. in Hepburn samples, compared to 0.31 to 0.65 a.p.f.u. in Bishop samples.

Fourth, slight but significant differences in the $Fe^{3+}/(Fe^{2+}+Fe^{3+})$ ratios are observed in the biotite of the two intrusive suites. In the Hepburn biotite, $Fe^{3+}/(Fe^{2+}+Fe^{3+})$ ratios vary from 0.04 to 0.09, compared to 0.09 to 0.18 for biotite in the Bishop suite.

In several of the Hepburn rocks (rocks units Hg2 and Ht1, samples L14, L609, S29 and S54 in Table 1), the biotite defines a good planar fabric and is a metamorphic mineral. Despite this, these biotite samples have compositional features that are identical to the biotite of the younger, undeformed rocks. This is probably because in this orogen, the older plutons are synmetamorphic, *i.e.*, were deformed during crystallization and emplacement, and were not subjected to a separate, later regional metamorphic event. Furthermore, the metamorphic fluids that catalyzed the recrystallization of the biotite in the older foliated rocks were probably exsolved from the plutons during crystallization. In some cases, the biotite displays textural evidence of minor deuteric recrystallization, but this process does not seem to have promoted major compositional changes. For example, important deficiencies in the octahedral positions, as observed by Konings *et al.* (1988) in biotite of the Abas granite in

TABLE 2. COMPOSITION OF BIOTITE IN THE BISHOP INTRUSIVE SUITE

ROCK-UNIT[1]	Bg	Bg	Bg	Bg	Bg	Bd	Bg	Bg	Bg	Bg	Bg
SAMPLE	L243	L246	L255	L313	L315	L316[2]	L515A[2]	L531	L601[2]	S200[2]	Z53
# OF ANALYSES[3]	4	7	12	8	6	7	4	3	5	5	4
SiO_2 wt.%	34.97	36.11	35.51	37.29	36.93	38.47	36.34	36.54	34.11	33.13	34.28
TiO_2	5.64	3.69	4.69	2.73	3.02	4.58	3.28	3.13	5.48	5.19	4.27
Al_2O_3	13.32	13.09	12.99	13.66	13.86	14.30	14.00	14.64	13.07	12.60	13.81
Fe_2O_3	3.03	3.17	2.33	3.41	3.34	1.96	3.23	3.47	3.53	5.17	3.97
FeO	19.98	17.40	20.41	14.27	16.52	10.41	17.15	16.75	18.75	27.45	17.20
MnO	0.22	0.35	0.24	0.41	0.39	0.07	0.32	0.34	0.23	0.41	0.35
MgO	9.76	11.38	9.78	13.20	12.37	17.42	12.12	11.10	10.58	2.84	11.30
CaO	0.02	0.01	0.02	0.03	0.03	0	0.01	0.03	0.02	0.01	0.01
Na_2O	0.08	0.05	0.09	0.07	0.07	0.14	0.05	0.06	0.17	0.13	0.08
K_2O	9.63	9.63	9.82	9.78	9.62	8.72	9.40	9.76	9.47	9.41	9.83
F	0.93	0.96	1.41	1.24	0.88	0.17	0.58	0.69	0.66	0.74	1.15
Cl	0.22	0.10	0.27	0.05	0.06	0.07	0.12	0.09	0.23	0.22	0.10
O≡F, Cl	0.44	0.43	0.65	0.53	0.38	0.09	0.28	0.31	0.33	0.36	0.50
TOTAL	97.36	95.51	96.91	95.61	96.71	96.22	96.32	96.29	95.97	96.94	95.85
Structural formulae based on 22 oxygens											
Si	5.376	5.575	5.506	5.658	5.583	5.577	5.524	5.554	5.306	5.365	5.320
Z=8 ^{IV}Al	2.414	2.382	2.374	2.342	2.417	2.423	2.476	2.446	2.396	2.405	2.525
^{IV}Ti	0.210	0.044	0.121	0	0	0	0	0	0.298	0.230	0.155
^{VI}Al	0	0	0	0.101	0.053	0.021	0.031	0.176	0	0	0
^{VI}Ti	0.442	0.384	0.426	0.312	0.343	0.499	0.375	0.358	0.343	0.402	0.344
Fe^{3+}	0.351	0.369	0.272	0.390	0.380	0.214	0.370	0.397	0.414	0.631	0.464
Fe^{2+}	2.570	2.247	2.647	1.811	2.090	1.262	2.179	2.130	2.439	3.717	2.232
Mn	0.029	0.046	0.032	0.052	0.050	0.008	0.042	0.044	0.031	0.056	0.047
Mg	2.238	2.619	2.260	2.985	2.789	3.764	2.746	2.514	2.453	0.685	2.614
ΣY	5.629	5.664	5.636	5.651	5.705	5.769	5.742	5.61	5.680	5.491	5.701
Ca	0.003	0.001	0.003	0.005	0.005	0	0.002	0.004	0.004	0.002	0.001
Na	0.025	0.015	0.028	0.022	0.022	0.039	0.015	0.017	0.050	0.040	0.024
K	1.889	1.898	1.943	1.894	1.855	1.613	1.823	1.893	1.879	1.944	1.946
ΣX	1.918	1.914	1.975	1.921	1.882	1.652	1.841	1.914	1.933	1.986	1.971
F	0.451	0.470	0.691	0.595	0.418	0.077	0.280	0.330	0.327	0.381	0.564
Cl	0.057	0.025	0.071	0.012	0.015	0.018	0.031	0.023	0.060	0.061	0.026
Fe/(Fe+Mg)	0.566	0.500	0.563	0.424	0.470	0.282	0.481	0.501	0.538	0.864	0.508
$Fe^{3+}/(Fe^{2+}+Fe^{3+})$	0.120	0.141	0.093	0.177	0.154	0.145	0.145	0.157	0.145	0.145	0.172
Al tot.	2.414	2.382	2.374	2.443	2.470	2.443	2.507	2.622	2.396	2.405	2.525

[1] Rock units as defined in St-Onge et al. (1988):
Bd Orthopyroxene–hornblende diorite, quartz diorite; minor gabbro; accessory biotite and actinolite; massive.
Bg Biotite–hornblende monzogranite, syenogranite; minor granodiorite; K-feldspar megacrysts common; generally massive, pink.
[2] FeO/Fe_2O_3 estimated from analyses of biotite in the same rock unit.
[3] Number of analyses included in mean.

northern Portugal, and ascribed to muscovitization or chlorite interleaving, are not observed. Occupancies of the octahedral positions range from 5.49 to 5.77 a.p.f.u., corresponding to typical values of fresh biotite. However, small-scale homogenization of trace constituents like Rb and Sr, such as documented in the biotite of the Ploumanac'h complex (Barrière & Cotten 1979), cannot be ruled out.

In the Fe^{2+}–Fe^{3+}–Mg^{2+} diagram of Wones & Eugster (1965), biotite compositions from the Hepburn suite define an elongate cluster that falls between the quartz – fayalite – magnetite (QFM) and Ni–NiO (NNO) oxygen fugacity buffers (Fig. 6). Biotite in the Bishop suite appears to have been buffered, but at slightly higher fugacities of oxygen, from the NNO buffer up to the hematite–magnetite curve (HM) (Fig. 6). A better evaluation of oxygen fugacity can be made from the Fe/(Fe+Mg) ratio of the biotite by using the calibrated curves of Wones & Eugster (1965) in $f(O_2)$–T space for the biotite + K-feldspar + magnetite equilibrium (Fig. 7). These three phases coexist in all granitic rocks of the Bishop intrusive suite. If we disregard sample S200 and assume a reasonable temperature of crystallization of 800°C for these granitic rocks, the Bishop rocks equilibrated at an oxygen fugacity between $10^{-11.9}$ and $10^{-13.9}$ bars [Fe/(Fe+Mg) = 0.42 to 0.57], which corresponds to conditions at or above the NNO buffer.

Similarly, the biotite from the Hepburn granites would have equilibrated at an oxygen fugacity between $10^{-14.3}$ and $10^{-15.8}$ bars [Fe/(Fe+Mg) = 0.61 to 0.78], close to the QFM buffer. In these rocks, however, magnetite is conspicuously absent; thus the biotite → K-feldspar + magnetite reaction did not buffer the fugacity of oxygen. The oxygen fugacities suggested for both suites by this method nevertheless correspond to those from Figure 6.

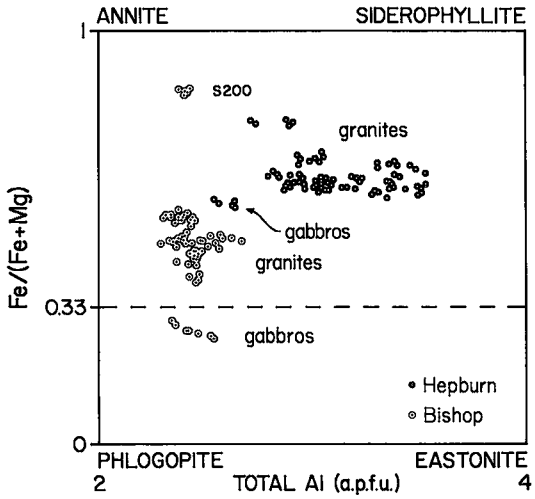

FIG. 5. Plot of Fe/(Fe+Mg) *versus* total Al in biotite from the Hepburn and Bishop intrusive suites. Note how the biotite from the gabbros of both suites plot separately in the biotite quadrilateral from the biotite from granites.

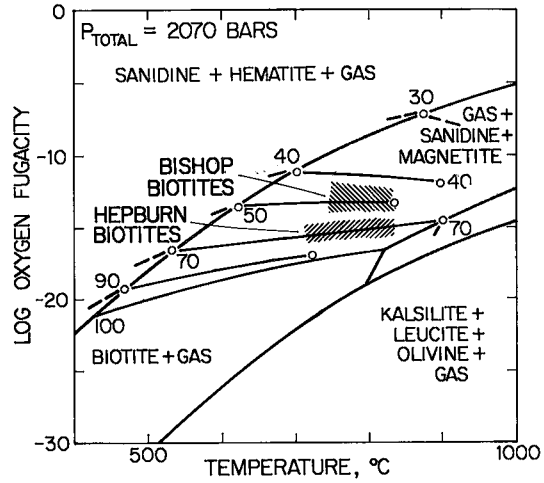

FIG. 7. Log $f(O_2)$ – T diagram for the biotite + sanidine + magnetite + gas equilibrium at P_{tot} = 2070 bars (from Wones & Eugster 1965). Illustrated are Fe/(Fe+Mg) isopleths. Ruled patterns represent range of oxygen fugacity for biotite samples from the Hepburn and Bishop suites assuming an equilibrium temperature of approximately 800°C.

In their original work, Wones & Eugster (1965) recognized two contrasting trends in the $f(O_2)$–T diagram (Fig. 7): an oxidizing trend, in which biotite becomes increasingly Mg-rich with falling temperature (or progressing crystallization), and a reducing trend, in which biotite becomes increasingly Fe-rich. In Figure 8, the solidification index $100MgO/(MgO + FeO + Fe_2O_3 + Na_2O + K_2O)$ was substituted for temperature. In this diagram, the Hepburn intrusive suite shows a trend of moderate iron-enrichment with progressing crystallization (decreasing solidification index) that is mimicked by its biotite (Fig. 8A). The Bishop suite also defines a trend of Fe-enrichment that is slightly steeper; however, its biotite values are more scattered and show an overall decrease. This indicates that $f(O_2)$ must have increased with progressive crystallization, partitioning iron into Fe^{3+}-bearing phases such as magnetite rather than mafic silicate minerals. Similar trends of oxidation have been recorded in biotite of Japanese plutonic rocks (Murakami 1969) and have contributed to the recognition of the ilmenite- and magnetite-series granitic rocks of Ishihara (1981).

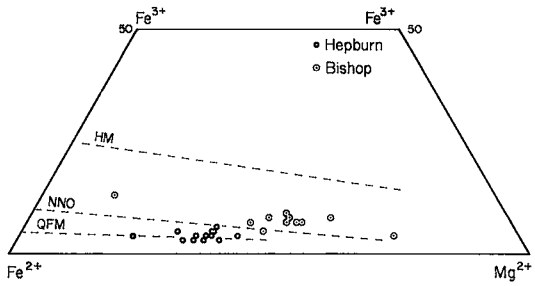

FIG. 6. Fe^{2+}–Fe^{3+}–Mg diagram of Wones & Eugster (1965). Biotite from the Hepburn suite clusters near the QFM buffer, whereas biotite from the Bishop suite clusters at or above the NNO buffer.

COLOR OF BIOTITE

One of the most distinctive petrographic features of the Hepburn and Bishop intrusive suites is the difference in the pleochroic colors of their biotite. The examination of over 300 thin sections revealed that over 95% of all the biotite in the Hepburn suite is reddish brown to bright fire-red along the *Y* or *Z* directions (Fig. 4A), whereas in the Bishop suite, biotite is greenish brown to green along the same directions (Fig. 4B).

The transmission spectra of all the biotite samples have, at first glance, an overall similarity; they are all characterized by maximum transmission in the near-infrared, from 810 to 830 nm, and minimum transmission in the violet to green segment, from 470 to 550 nm (Fig. 9). However, a closer look reveals significant differences. In the range from approximately 660 to 750 nm, corresponding to the red part of the visible spectrum,

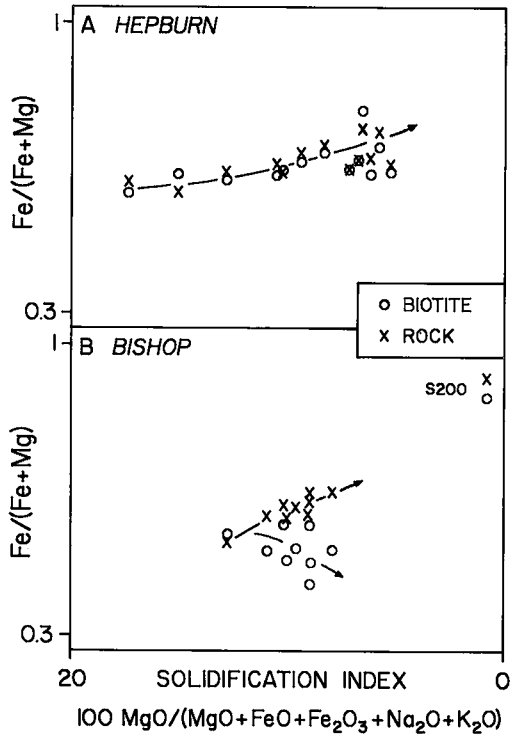

FIG. 8. Evolution of whole-rock Fe/(Fe+Mg) values and corresponding values in biotite with progressing crystallization (as represented by the solidification index) for the Hepburn suite (A) and Bishop suite (B). In the Hepburn suite, whole rock and biotite define overlapping Fe-enrichment trends. In contrast, biotite in the Bishop rocks seems to undergo Mg-enrichment with progressing crystallization despite whole-rock Fe-enrichment.

biotite from the Hepburn suite has considerably higher transmission than that in the Bishop samples. Correspondingly, the Bishop biotite has higher intensity of transmission in the 520 to 630 nm segment of the spectrum, roughly corresponding to green and yellow. The mean spectra of the two suites further illustrate this difference; the transmittances intersect at 650 nm (Fig. 9). Below 650 nm, in the green, Hepburn biotite transmits less than Bishop biotite; above 650 nm, in the red, the reverse is true.

The relationships between color and composition in biotite are complex and have been considered only qualitatively in most studies. Hall (1941) correlated the color of biotite as observed in thin sections with concentrations of FeO_{total}, MgO and TiO_2. He concluded that high iron and titanium contents are responsible for the green and red colors, respectively. This is the contrary of what is found here: the most Fe-rich biotite (Hepburn) is reddish, and the most Ti-rich biotite (Bishop) is green. In a study similar to Hall's (1941), but more detailed, Hayama (1959) compiled the colors of 96 specimens of biotite. He concluded that high contents of Ti are responsible for the red color and stressed that high $Fe_2O_3/(FeO+Fe_2O_3)$ values cause the green color. He also concluded that Mg-contents are irrelevant in this respect. Our results seem to agree, in part, with Hayama's findings. Certainly, our most Fe^{3+}-rich biotite samples, from the Bishop suite, are green. However, according to his compositional criteria, the biotite in most of the Bishop samples, with its relatively high Ti content, should be red rather than green.

More recent spectroscopic studies have focused on the assignments of absorption bands to specific cations or cation interactions. Fe^{2+} or Fe^{2+}–Fe^{3+} interactions are believed responsible for three absorption bands lying in the red to near-infrared (720, 920 and 1150 nm) (Faye 1968, Marfunin *et al.* 1969, Bakhtin & Vinokurov 1978, Smith 1978, Kliem & Lehmann 1979, Smith *et al.* 1980).

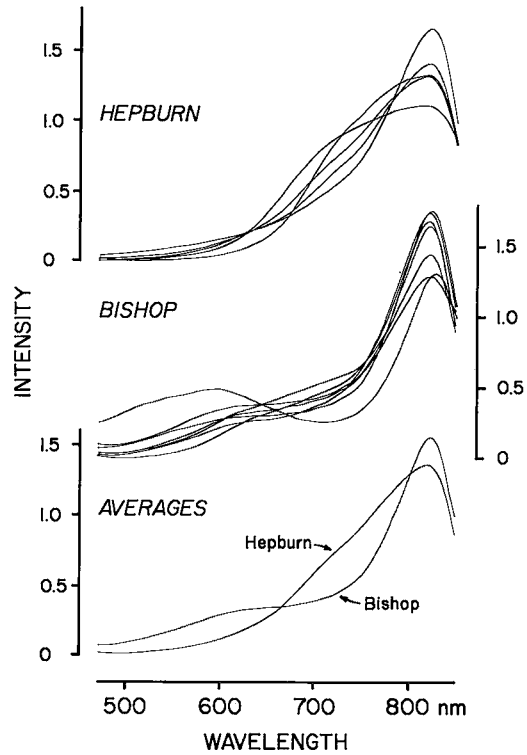

FIG. 9. Optical transmission spectra of biotite samples from Hepburn rocks, and biotite samples from Bishop rocks; also shown are averages for both suites.

Absorption at 400 nm, in the violet end of the spectrum, has been ascribed to a Fe^{2+}–Ti^{4+} interaction (Faye 1968).

Our data suggest that the oxidation state of iron and the Fe/(Fe+Mg) ratio, inasmuch as this ratio is also a function of the oxidation state of iron, exert some control on the color of biotite. The role played by Ti, however, is not clear since our most Ti-rich material, from the Bishop suite, is green. In a study of biotite from the Adamello massif, DePieri & Jobstraibizer (1977) concluded that Ti-contents are not responsible for the change from greenish brown to red absorption colors. The reduced form of Ti (Ti^{3+}) may play a role as important as absolute abundance of Ti in causing the red color. The occurrence of Ti^{3+} has been suggested in red biotite from reduced metamorphic rocks (Gorbatschev 1972), but remains to be demonstrated.

As a generalization, red biotite is Fe-rich, has low $Fe^{3+}/(Fe^{2+}+Fe^{3+})$ values and is Ti-bearing, although total abundances of Ti need not be high. It is characteristic of reduced, generally peraluminous granitic rocks. Green or greenish brown biotite is Mg-rich and has a higher $Fe^{3+}/(Fe^{2+}+Fe^{3+})$. It occurs more commonly in oxidized metaluminous granitic rocks. In the dominantly metaluminous rocks of the calc-alkaline Sierra Nevada batholith, Dodge *et al.* (1969) found nearly all samples of biotite to be olive, green or brown. One of their few exceptions, a red biotite (sample FD–20), is from a peraluminous two-mica granodiorite. In the Sithonia igneous complex in Greece, Sapountzis (1976) found the biotite from biotite–muscovite granites and granodiorites to be brown, in contrast to the brownish green and olive-green biotite from hornblende-bearing granodiorites. Similar associations of red and green biotite have also been observed in, respectively, reduced and oxidized metamorphic rocks from Maine (Dyar 1990) and Scotland (Chinner 1960).

Biotite and the Classification of Granitic Rocks

The most pronounced compositional characteristics of the biotite in the Hepburn and Bishop intrusive suites are their differences in total Al contents and in Fe/(Fe+Mg) values. Both features are sensitive indicators of conditions that prevailed in the host magmas. The total Al content of biotite reflects directly the peraluminosity of the host magma. This is evident on a plot of biotite peraluminosity *versus* whole-rock peraluminosity for all the samples (Fig. 10). Compositions of Hepburn biotite show a clear positive correlation between A/CNK values for the biotite and for the whole rock. This is because biotite commonly hosts excess aluminum in peraluminous granites (Speer 1984). Muscovite, garnet and sillimanite could also greatly contribute to the peraluminosity of the rocks, but in the Hepburn as in many other peraluminous granites, these phases occur only as accessories, and biotite is the most abundant peraluminous mineral. Similar relationships

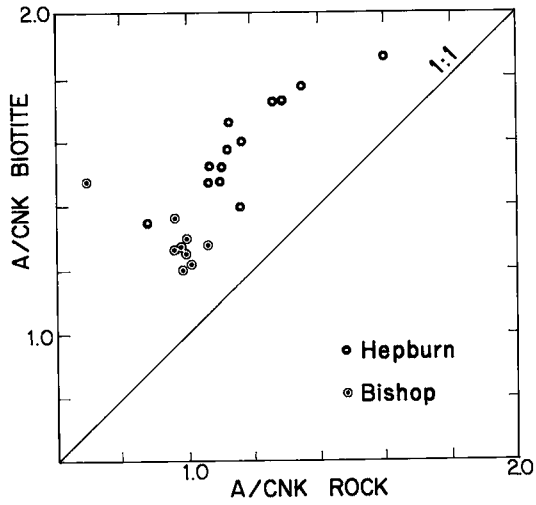

FIG. 10. Plot of peraluminosity index (A/CNK) of biotite *versus* that of whole-rock samples.

have been documented in biotite from granites of northern Portugal (de Albuquerque 1973) and in the Clouds Creek pluton of South Carolina (Speer 1981).

Similarly, the Fe/(Fe+Mg) values of biotite from the Hepburn and Bishop reflect important differences in the oxygen fugacity of these two plutonic suites. Biotite from the granites of the Hepburn suite evolved at or near the QFM buffer, under considerably more reducing conditions than those recorded for the Bishop granites, which evolved at, or above, the NNO buffer.

These features are ideally portrayed in the annite – siderophyllite – phlogopite – eastonite quadrilateral, commonly used to plot the compositions of trioctahedral micas in terms of total aluminum (a.p.f.u.) and Fe/(Fe+Mg).In this plot (Fig. 5), biotite samples from the Hepburn and Bishop suites define two distinct and non-overlapping fields. The Hepburn field is characterized by Fe-rich compositions, a relatively narrow range of Fe/(Fe+Mg) values (note that biotite from the gabbros is only slightly more Mg-rich than that in the granites), and a pronounced trend of increasing total Al from ~ 2.61 a.p.f.u. in the gabbros to 3.52 a.p.f.u. in the granites. The Bishop field shows exactly the opposite; compositions are more Mg-rich, and there is a wide range of Fe/(Fe+Mg) values at relatively constant Al contents. Fe/(Fe+Mg) values of biotite in the Bishop suite vary from 0.28 in the gabbros to a maximum of 0.57 in the granites, a range considerably greater than that in the Hepburn suite. Note that in both intrusive suites, there is a significant compositional gap between the biotite of the gabbros and granites. This is probably because most of the biotite in the gabbros is secondary, and its composition is inherited from the Mg-rich clinopyroxene it replaces.

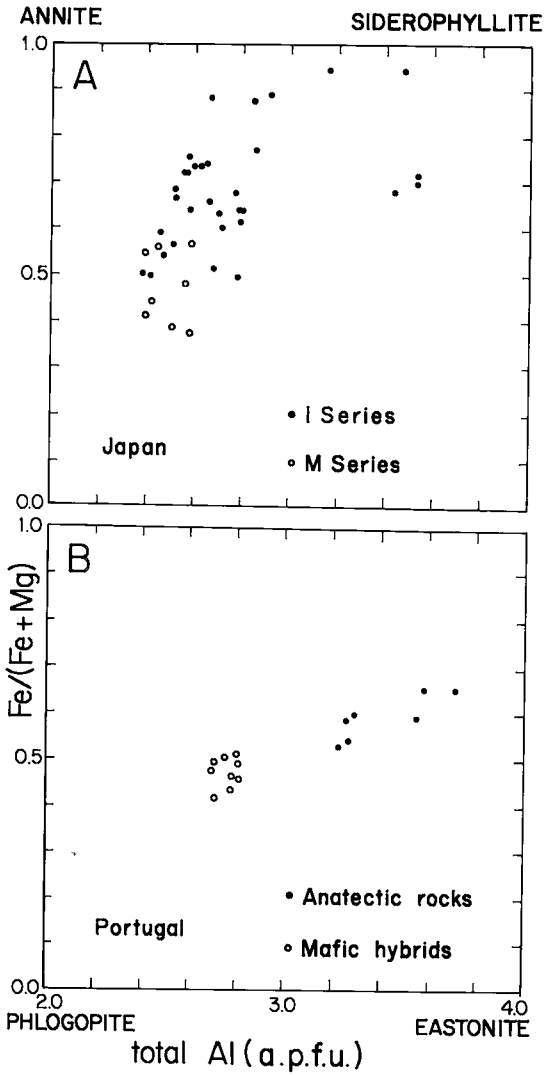

FIG. 11. A) Biotite quadrilateral showing samples from the Japanese I- (solid circles) and M-series (open circles) granites (data from Czamanske *et al.* 1981). B) Composition of biotite samples from the Aregos Hercynian granites of northern Portugal (data form de Albuquerque 1973); open circles represent biotite from mafic hornblende–biotite hybrids, and solid circles represent biotite from felsic anatectic granites.

It is informative to compare the biotite trends of the Wopmay granites in the biotite quadrilateral with those of well-known granites. For example, the biotite compositions from the ilmenite- and magnetite-series granites of the Inner Zone batholith in Japan (Czamanske *et al.* 1981) define a continuum from the M-series, with the most Mg-rich and Al-poor mica, to the I-series with increasing Fe- and Al-contents (Fig. 11A). The continuity of the trend, and the partial overlapping of the I- and M-series fields, suggest that both granitic series resulted from a common magmatic event but with varying proportions of involvement of metasedimentary material. The achievement of extremely Fe-rich compositions at only intermediate Al values in micas of the I-series granites implies that these magmas became rapidly reduced before arriving to high peraluminosity.

In the Aregos region of northern Portugal, Hercynian granites have been subdivided into two genetically distinct suites (de Albuquerque 1973). These are mafic hybrids composed of hornblende–biotite tonalites and granodiorites and felsic anatectic granitic rocks composed of peraluminous biotite–muscovite granodiorites and granites. The mica from these two suites defines two distinct, non-overlapping fields in the biotite quadrilateral (Fig. 11B), corroborating the distinct petrogenetic origins proposed for these rocks by de Albuquerque (1973). Unlike the Japanese rocks, none of the Aregos granitic rocks seem to have been highly reduced, since the maximum Fe/(Fe+Mg) value encountered in the mica is only 0.66. The slope of the mica trends in the quadrilateral may well reflect the balance between the aluminum and graphite contents of the metasedimentary or crustal rocks involved in the genesis of their host magmas.

The Hepburn and Bishop intrusive suites and the plutons from Japan and Portugal all illustrate the value of the biotite quadrilateral in discriminating plutonic associations, especially where assimilation or anatexis of aluminous sediments and oxidation are involved. Both of these magmatic processes can in turn be associated to specific tectonic environments.

Strongly peraluminous magmas have been ascribed to numerous igneous mechanisms, such as anatexis of diopside-normative source rocks (Cawthorn *et al.* 1976), fractional crystallization (Ringwood 1974), and metasomatic loss of alkalis (Martin & Bowden 1981). However, the most commonly invoked process, and probably the one responsible for the bulk of peraluminous granites, is anatexis or assimilation of pelitic metasediments (Chappell & White 1974). Since anatexis and assimilation of metasedimentary material are mechanisms that both require considerable input of heat, many peraluminous granites are spatially and temporally associated with the important thermal culminations that follow crustal thickening in continental collision zones. These are the syn-collisional (SYN-COLG) granites of Pearce *et al.* (1984) or the continental collision granites (CCG) of Maniar & Piccoli (1989). Examples of such rocks include the Himalayan leucogranites (LeFort 1981, Debon *et al.* 1986) and the leucogranites of the South Armorican shear zone in Brittany (Strong & Hanmer 1981).

In the case of the Hepburn intrusive suite, recent studies (Lalonde 1989) suggest that although magmatism first originated in an arc-related setting, this tectonic environment rapidly evolved into a closing back-arc

basin, therefore a collisional setting, with an associated anatectic metamorphic event. Although it would be a serious oversimplification to claim that granites whose biotite defines a Al-enrichment trend in the biotite quadrilateral belong to continental collision zones, it is reasonable to interpret these trends as indications of important metasedimentary contributions to these granites, either by assimilation or anatexis.

Changes in the redox state of plutonic systems are not as well documented as changes in peraluminosity, principally because of the inherent difficulty in monitoring the oxygen fugacity of these systems. Magmatic reduction is an important process, especially in the genesis of peraluminous granites, where it is caused by the incorporation of or contamination by graphite-bearing metasediments (Ishihara 1981). Magmatic oxidation has been inferred in numerous plutons by Mg enrichments in the mafic silicates with progressive crystallization, presumably because of strong depletions of Fe^{2+} in the magmas. Several mechanisms of oxidation have been proposed, including the interaction of magmas with atmospheric oxygen (Haslam 1968), but the most commonly invoked has been the loss of protons following magma degassing (Czamanske & Wones 1973). This process, which implies that oxidation is a late-acquired feature, has been shown to be effective only in highly evolved water-rich and Fe-poor magmas (Candela 1986). Recently, Rowins *et al.* (1991) have demonstrated that the magmas of the Archean Murdock Creek syenite (Abitibi belt, Ontario) were oxidized at their source, presumably by fusion of an oxidized parent.

Most cases of strong magmatic oxidation are plutons with alkaline or anorogenic affiliations. Examples include the granites and monzonites of the Finnmarka complex (Czamanske & Mihálik 1972, Czamanske & Wones 1973), the Kauai alkali gabbro from Hawaii (Johnston & Stout 1984, Johnston *et al.* 1985) and the Baie-des-Moutons syenitic complex (Lalonde & Martin 1983). Although not necessarily as strongly oxidized, the rocks of the large continental arc batholiths, and their volcanic equivalents, also are known for their high Fe_2O_3/FeO values and oxidized nature (Ishihara 1977, Gill 1981). In these rocks, the mechanisms leading to high fugacities of oxygen are not always well understood.

In summary, peraluminous magmas are typical of continental collision zones, where they are generated in response to anatexis of metasedimentary rocks. Strongly oxidized magmas are rare and appear to be limited to anorogenic settings, whereas moderately oxidized rocks are typical of the more voluminous magmatism of continental arcs.

Conclusions

In the Hepburn internal zone of the early Proterozoic Wopmay orogen, the granitic rocks of the Hepburn and Bishop intrusive suites can easily be discriminated by the contrasting composition and color of their biotite. These compositional features are best displayed in the annite – siderophyllite – phlogopite – eastonite quadrilateral (biotite quadrilateral). In this diagram, the biotite from the Hepburn intrusive suite, a peraluminous continental collision suite with an important metasedimentary contribution, defines a trend of increasing Al contents at constant Fe/(Fe+Mg) values. In contrast, the biotite of the Bishop intrusive suite, a continental arc-related metaluminous suite, shows increasing Fe/(Fe+Mg) values at constant Al contents.

In many instances, the color of the biotite may also be useful. Red biotite is characteristic of many reduced peraluminous granites, in contrast to green or greenish brown biotite in arc-related suites. The red color appears to be caused by enrichment in both total Fe and Fe^{2+}. In addition, Ti, probably present as Ti^{3+}, may play a role. Green biotite is enriched in Mg and Fe^{3+}.

Acknowledgements

This research was supported by NSERC operating grants to Lalonde and Bernard. Additional support to Lalonde came from the Rector's Fund of the University of Ottawa. We thank Richard Ernst, Denis Rancourt and Steve Rowins for their reviews of a first draft of this paper, and L. Paul Bédard for bringing to our attention the work of Nachit *et al.* (1985). Field work associated with this project was made possible by the Geological Survey of Canada. Finally, J. Alex Speer, Robert F. Martin, and one anonymous referee are thanked for their constructive reviews.

References

Ague, J.J. & Brimhall, G.H (1988): Regional variations in bulk chemistry, mineralogy, and the compositions of mafic and accessory minerals in the batholiths of California. *Geol. Soc. Am. Bull.* **100**, 891-911.

Bakhtin, A.I. & Vinokurov, V.M. (1978): Exchange-coupled pairs of transition metal ions and their effect on the optical absorption spectra of rock-forming silicates. *Geochem. Int.* **15**(1), 53-60.

Barbarin, B. (1990): Granitoids: main petrogenetic classifications in relation to origin and tectonic setting. *Geol. J.* **25**, 227-238.

Barrière, M. & Cotten, J. (1979): Biotites and associated minerals as markers of magmatic fractionation and deuteric equilibration in granites. *Contrib. Mineral. Petrol.* **70**, 183-192.

Candela, P.A. (1986): The evolution of aqueous vapor from silicate melts: effect on oxygen fugacity. *Geochim. Cosmochim. Acta* **50**, 1205-1211.

Cawthorn, R.G., Strong, D.F. & Brown, P.A. (1976): Origin

of corundum normative intrusive and extrusive magmas. *Nature* **259**, 102-104.

CHAPPELL, B.W. & WHITE, A.J.R. (1974): Two contrasting granite types. *Pac. Geol.* **8**, 173-174.

CHINNER, G.A. (1960): Pelitic gneisses with varying ferrous/ferric ratios from Glen Cova, Angus, Scotland. *J. Petrol.* **1**, 178-217.

CZAMANSKE, G.K., ISHIHARA, S. & ATKIN, S.A. (1981): Chemistry of rock-forming minerals of the Cretaceous–Paleocene batholith in southwestern Japan and implications for magma genesis. *J. Geophys. Res.* **86**, 10431-10469.

_____ & MIHÁLIK, P. (1972): Oxidation during magmatic differentiation, Finnmarka complex, Oslo area, Norway. 1. The opaque oxides. *J. Petrol.* **13**, 493-509.

_____ & WONES, D.R. (1973): Oxidation during magmatic differentiation, Finnmarka complex, Oslo area, Norway. 2. The mafic silicates. *J. Petrol.* **14**, 349-380.

DE ALBUQUERQUE, C.A.R. (1973): Geochemistry of biotites from granitic rocks, northern Portugal. *Geochim. Cosmochim. Acta* **37**, 1779-1802.

DEBON, F., LEFORT, P., SHEPPARD, S.M.F. & SONET, J. (1986): The four plutonic belts of the TransHimalaya – Himalaya: a chemical, mineralogical, isotopic and geochronological synthesis along a Tibet – Nepal section. *J. Petrol.* **27**, 219-250.

DEER, W.A., HOWIE, R.A. & ZUSSMAN, J. (1962): *Rock-Forming Minerals*. **3**. *Sheet Silicates*. Longmans, London.

DE PIERI, R. & JOBSTRAIBIZER, P.G. (1977): On some biotites from Adamello massif (Northern Italy). *Neues. Jahrb. Mineral. Monatsh.*, 15-24.

DODGE, F.C.W., SMITH, V.C. & MAYS, R.E. (1969): Biotites from granitic rocks of the central Sierra Nevada batholith, California. *J. Petrol.* **10**, 250-271.

DYAR, M.D. (1990): Mössbauer spectra of biotite from metapelites. *Am. Mineral.* **75**, 656-666.

FAYE, G.H. (1968): The optical absorption spectra of iron in six-coordinate sites in chlorite, biotite, phlogopite and vivianite. Some aspects of pleochroism in the sheet silicates. *Can. Mineral.* **9**, 403-425.

GILL, J.B. (1981): *Orogenic Andesites and Plate Tectonics*. Springer-Verlag, Berlin.

GORBATSCHEV, R. (1972): Coexisting varicolored biotites in migmatitic rocks and some aspects of element distribution. *Neues Jahrb. Mineral. Abh.* **118**, 1-22.

HALL, A.J. (1941): The relation between colour and chemical composition in the biotites. *Am. Mineral.* **26**, 29-33.

HASLAM, H.W. (1968): The crystallization of intermediate and acid magmas at Ben Nevis, Scotland. *J. Petrol.* **9**, 84-104.

HAYAMA, Y. (1959): Some considerations on the color of biotite and its relation to metamorphism. *J. Geol. Soc. Japan* **65**, 21-30.

HILDEBRAND, R.S., HOFFMAN, P.F. & BOWRING, S.A. (1987): Tectono-magmatic evolution of the 1.9 Ga Great Bear magmatic zone, Wopmay orogen, northwestern Canada. *J. Volcanol. Geotherm. Res.* **32**, 99-118.

HOFFMAN, P.F. & BOWRING, S.A. (1984): Short-lived 1.9 Ga continental margin and its destruction, Wopmay orogen, northwestern Canada. *Geology* **12**, 68-72.

_____, TIRRUL, R., KING, J.E., ST-ONGE, M.R. & LUCAS, S.B. (1988): Axial projections and modes of crustal thickening, eastern Wopmay orogen, northwest Canadian shield. *In* Processes in Continental Lithospheric Deformation (S.P. Clark, Jr., B.C. Burchfiel & J. Suppe, eds.). *Geol. Soc. Am., Spec. Pap.* **218**, 1-29.

ISHIHARA, S. (1977): The magnetite-series and ilmenite-series granitic rocks. *Mining Geol.* **27**, 293-305.

_____ (1981): The granitoid series and mineralization. *Econ. Geol., 75th Anniv. Vol.*, 458-484.

JOHNSTON, A.D. & STOUT, J.H. (1984): A highly oxidized ferrian salite-, kennedyite-, forsterite-, and rhönite-bearing alkali gabbro from Kauai, Hawaii and its mantle xenoliths. *Am. Mineral.* **69**, 57-68.

_____, _____ & MURTHY, V.R. (1985): Geochemistry and origin of some unusually oxidized alkaline rocks from Kauai, Hawaii. *J. Volcanol. Geotherm. Res.* **25**, 225-248.

KING, J.E. (1986): The metamorphic internal zone of Wopmay orogen (early Proterozoic), Canada: 30 km of structural relief in a composite section based on plunge projection. *Tectonics* **5**, 973-994.

KLIEM, W. & LEHMANN, G. (1979): A reassignment of the optical absorption bands in biotites. *Phys. Chem. Minerals* **4**, 65-75.

KONINGS, R.J.M., BOLAND, J.M., VRIEND, S.P. & JANSEN, J.B.H. (1988): Chemistry of biotites and muscovites in the Abas granite, northern Portugal. *Am. Mineral.* **73**, 754-765.

LALONDE, A.E. (1986): *The Intrusive Rocks of the Hepburn Metamorphic – Plutonic Zone of the Central Wopmay Orogen, N.W.T.* Ph.D. thesis, McGill University, Montreal, Quebec.

_____ (1989): Hepburn intrusive suite: peraluminous plutonism within a closing back-arc basin, Wopmay orogen, Canada. *Geology* **17**, 261-264.

_____ & MARTIN, R.F. (1983): The Baie-des-Moutons syenitic complex, La Tabatière, Québec. II. The ferromagnesian minerals. *Can. Mineral.* **21**, 81-91.

_____ & RANCOURT, D.G. (1990): Accuracy of Mössbauer and wet-chemistry Fe^{3+}/Fe^{2+} determinations in biotite: implications for mineralogical and petrological studies. *Geol.*

Assoc. Can. – Mineral. Assoc. Can., Program Abstr. **15**, A71-A72.

LE FORT, P. (1981): Manaslu leucogranite: a collision signature of the Himalaya – a model for its genesis and emplacement. *J. Geophys. Res.* **86**, 10545-10568.

MANIAR, P.D. & PICCOLI, P.M. (1989): Tectonic discrimination of granitoids. *Geol. Soc. Am. Bull.* **101**, 635-643.

MARFUNIN, A.S., MINEYEVA, R.M., MKRTCHYAN, A.R., NYUSSIK, YA.M. & FEDEROV, V.YE. (1969): Optical and Mössbauer spectroscopy of iron in rock-forming silicates. *Int. Geol. Rev.* **11**, 31-44.

MARTIN, R.F. & BOWDEN, P. (1981): Peraluminous granites produced by rock – fluid interaction in the Ririwai nonorogenic ring-complex, Nigeria: mineralogical evidence. *Can. Mineral.* **19**, 65-82.

MURAKAMI, N. (1969): Two contrastive trends of evolution of biotite in granitic rocks. *J. Jap. Assoc. Mineral. Petrol. Econ. Geol.* **62**, 223-248.

NACHIT, H., RAZAFIMAHEFA, N., STUSSI, J.M. & CARRON, J.-P. (1985): Composition chimique des biotites et typologie magmatique des granitoïdes. *C.R. Acad. Sci., Sér.* **II, 301**, 813-818.

PEARCE, J.A., HARRIS, N.B.W. & TINDLE, A.G. (1984): Trace element discrimination diagrams for the tectonic interpretation of granitic rocks. *J. Petrol.* **25**, 956-983.

PHILLIPS, E.R. & RICKWOOD, P.C. (1975): The biotite – prehnite association. *Lithos* **8**, 275-281.

RANCOURT, D.G., DANG, M.-Z. & LALONDE, A.E. (1992): Mössbauer spectroscopy of tetrahedral Fe^{3+} in trioctahedral micas. *Am. Mineral.* **77**, 34-43.

RINGWOOD, A.E. (1974): The petrological evolution of island arc systems. *J. Geol. Soc. London* **130**, 183-204.

ROWINS, S.M., LALONDE, A.E. & CAMERON, E.M. (1991): Magmatic oxidation in the syenitic Murdock Creek intrusion, Kirkland Lake, Ontario: evidence from the ferromagnesian minerals. *J. Geol.* **99**, 395-414.

ST-ONGE, M.R. & KING, J.E. (1987): Evolution of regional metamorphism during back-arc stretching and subsequent crustal shortening in the 1.9 Ga Wopmay orogen, Canada. *Philos. Trans., R. Soc. London* **A321**, 199-218.

_____, _____ & LALONDE, A.E. (1988): Geology, east-central Wopmay orogen, Northwest Territories. *Geol. Surv. Can., Open-File Rep.* **1923**.

SAPOUNTZIS, E.S. (1976): Biotites from the Sithonia igneous complex (North Greece). *Neues Jahrb. Mineral. Abh.* **126**, 327-341.

SMITH, G. (1978): Evidence for absorption by exchange-coupled Fe^{2+}–Fe^{3+} pairs in the near infra-red spectra of minerals. *Phys. Chem. Minerals* **3**, 375-383.

_____, HOWES, B. & HASAN, Z. (1980): Mössbauer and optical spectra of biotite: a case for Fe^{2+}–Fe^{3+} interactions. *Phys. Status Solidi* **A57**, K187-K192.

SPEER, J.A. (1981): Petrology of cordierite- and almandine-bearing granitoid plutons of the southern Appalachian Piedmont, U.S.A. *Can. Mineral.* **19**, 35-46.

_____ (1984): Micas in igneous rocks. *In* Micas (S.W. Bailey, ed.). *Rev. Mineral.* **13**, 299-356.

STRONG, D.F. & HANMER, S.K. (1981): The leucogranites of Southern Brittany: origin by faulting, frictional heating, fluid flux and fractional melting. *Can. Mineral.* **19**, 163-176.

WILSON, A.D. (1955): A new method for the determination of ferrous iron in rocks and minerals. *Geol. Surv. Great Britain, Bull.* **9**, 56-58.

WONES, D.R. & EUGSTER, H.P. (1965): Stability of biotite: experiment, theory, and application. *Am. Mineral.* **50**, 1228-1272.

Received November 21, 1991, revised manuscript accepted June 30, 1992.

APPENDIX 1. ACCURACY AND REPRODUCIBILITY OF MICROPROBE ANALYSES REPEATED ANALYSES OF BIOT STANDARD[1]

COMPILED FROM 17 DETERMINATIONS		MIN.	MAX.	STD. DEV.	AVGE	RECOGNIZED VALUES
SiO_2	wt.%	35.58	39.26	0.234	38.20	38.33
TiO_2		1.01	2.29	0.092	1.61	1.67
Al_2O_3		14.70	16.04	0.090	15.44	15.30
FeO[2]		8.97	11.66	0.209	10.17	10.36
MnO		0.04	0.22	0.009	0.11	0.11
MgO		17.03	20.57	0.279	19.40	19.35
CaO		0	0.24	0.017	0.04	0.05
Na_2O		0.04	0.11	0.005	0.07	0.09
K_2O		8.56	10.75	0.208	9.53	10.03
F		0	0.84	0.058	0.39	0.26
Cl		0	0.05	0.005	0.02	?

[1] Compilation of minimum values (MIN.), maximum values (MAX.), standard deviations (STD. DEV.), averages (AVGE) and recognized values of all the element analyzed for on the BIOT standard (Taylor Corp., Stanford, California) over a period of 4 years.

[2] All Fe assumed to be FeO